Proceedings of the International Heat Transfer Conference
IHTC14
August 8-13, 2010, Washington, DC, USA

IHTC14-23020

Experimental Heat Transfer Enhancement in Single-phase Liquid Microchannel Cooling with Cross-flow Synthetic Jet

Ruixian Fang[1], Wei Jiang[1], Jamil Khan[1], Roger Dougal[2]

Department of Mechanical Engineering[1] and Department of Electrical Engineering[2]
University of South Carolina, Columbia, SC, USA

ABSTRACT

The present study experimentally investigated a new hybrid cooling scheme by combination of a microchannel heat sink with a micro-synthetic jet actuator. The heat sink consisted of a single rectangular microchannel measured 550 μm wide, 500 μm deep and 26 mm long. The synthetic jet actuator with a 100 μm diameter orifice was placed right above the microchannel and 5 mm downstream from the channel inlet. Micro jet is synthesized from the fluid flowing through the microchannel. Periodic disturbance is generated when the synthetic jet interacts with the microchannel flow. Heat transfer performance is enhanced as local turbulence is generated and propagated downstream the microchannel. The scale and frequency of the disturbance can be controlled by changing the driving voltage and frequency of the piezoelectric driven synthetic jet actuator. The effects of synthetic jet on microchannel heat transfer performance were studied based on the microchannel flow Reynolds number, the jet operating voltage and frequency, respectively. It shows that the synthetic jet has a greater heat transfer enhancement for microchannel flow at lower Reynolds number. It also shows that the thermal effects of the synthetic jet are functions of the jet driving voltage and frequency. We obtained around 42% heat transfer enhancement for some test cases, whereas the pressure drop across the microchannel increases very slightly. The paper concludes that the synthetic jet can effectively enhance single-phase liquid microchannel heat transfer performance and would have more promising enhancements if multi-jets are applied along the microchannel.

Keywords: synthetic jet, microchannel, heat transfer enhancement

1. INTRODUCTION

With advancements in micro-processors and other high power electronics, the need for high heat flux removal has grown more critical owing to the increase in the total heat generation rate, and the heat generation rate per unit area. Some of the applications require heat flux well above 100 W/cm^2. Many advanced cooling solutions have been examined in recent years for the thermal management of high power density electronics. Of these cooling schemes, microchannel cooling and jet-impingement cooling are considered the two most effective solutions for devices demanding very high heat flux removal [1]. Bergles [2] presented the fourth generation of heat transfer enhancement using a combination of different techniques. This suggestion can be extended to microscale heat transfer augmentation. Present study experimentally explored the possibility to enhance the single-phase microchannel heat transfer by a hybrid cooling scheme, which combines the microchannel cooling with micro-synthetic jet-impingement cooling.

Single-phase liquid cooling in microchannels has shown considerable promise for removal of large amount of heat from a small area. There are over hundred papers that address the single-phase flow of liquids in microchannels. The most well-known work, by Tuckerman and Pease [3], is often considered to be the pioneering study of introducing the concept of microchannels for electronics cooling. They employed the direct circulation of water in microchannels fabricated into a 1.0 x 1.0 cm^2 silicon chip. Their heat sink can dissipate heat fluxes as high as 790 W/cm^2 with a maximum substrate temperature to inlet water temperature difference of 71^{o}C. The flow regime is highly turbulent for their case. However the benefits were tempered by the increased pressure drop, it was as large as 200kPa with the plain microchannels.

For microchannel flow under a lower pressure drop, further increase in microchannel heat transfer coefficient is very desirable for accommodating higher heat fluxes. Heat transfer enhancement can be achieved by interrupting boundary layer through the means of passive ways such as various channels configurations presented by Steinke and Kandlikar [4]. Colgan et al. [5] also provided a practical implementation of offset strip-fin enhanced microchannels and obtained significantly higher heat transfer coefficient, but with the penalty of pressure drop of around 35 kPa.

The present study provides an active way to enhance the microchannel heat transfer coefficient by interrupting the boundary layer through the means of a synthetic jet, which will periodically generate disturbance into the channel flow and make the flow turbulent. Heat transfer is enhanced as the result of the generated turbulence and its propagation downstream of the microchannel. While the pressure drop across the microchannel stays almost the same.

Synthetic jet is a novel method for active flow control which has been demonstrated by Glezer and Amitay [6]. The method uses a small actuator which synthesizes a jet from the flow that is being controlled without the need for mass injection. It requires no input piping and complex fluidic packaging, only electric power.

A synthetic jet actuator, in general, consists of an enclosed cavity with one side of the cavity having an orifice while a flexible membrane located on the opposite side to the orifice. The jet is generated at the orifice by oscillating the membrane. Working fluid is sucked into the cavity and then rapidly expelled out. As the outgoing flow passes the sharp edges of the orifice, the flow separates forming a vortex ring, which propagates into the ambient fluid. An important feature of synthetic jets is that they are zero-net-mass-flux in nature (Glezer and Amitay [6]), since they are synthesized from ambient fluid. As such, synthetic jets allow momentum transfer into the surrounding fluid without net mass injection into the overall system. This attribute makes synthetic jets ideally suited for fabrication using micromachining techniques that enable low cost fabrication, realization of large arrays, and the potential for integration of control electronics.

For thermal management applications, synthetic jets impinging directly on electronics have been investigated for many years. Recently, the focus has moved away from impingement jets to jets acting in a pre-existing flow [7]. This topic has been studied extensively for active flow control applications in areas including jet vectoring (Smith and Glezer [8]), separation control of both external and internal flows (Amitay et al. [9], Crook et al. [10]), but little exists on the thermal effects of a jet interacting with a crossing flow.

Mahalingam and Glezer [11] studied air cooled plate-fin heat sinks augmented with synthetic jet arrays. They studied the performance of a synthetic jet acting aligned with a channel. Each fin of the heat sink was straddled by a pair of synthetic jet that entrains cool ambient air upstream of the heat sink and discharges it into the channels between the fins. The test results shows that the synthetic jet heat sink dissipates ~40% more heat compared to steady flow from a ducted fan blowing air through the heat sink.

A numerical study of enhanced microchannel cooling using a synthetic jet actuator with air as working fluid was performed by Timchenko et al. [12]. A two-dimensional microchannel 200 μm high and 4.2 mm long was considered with top surface hot and all other walls being adiabatic. A slot synthetic jet is normal to the channel flow. The synthetic jet operated at 10 kHz with the amplitude of 42 μm. An assumed parabolic motion of the vibrating diaphragm was explicitly modeled. Unsteady compressible laminar model was employed. They studied the performance of the jet impinging on the opposite wall and showed that 64% improvement in cooling was possible though it largely depend on the size of the synthetic jet as well as the bulk channel flow condition.

Instead of air, Timchenko et al. [13] further numerically investigate heat transfer enhancement using synthetic jet actuator in forced convection water filled microchannels. Again, unsteady computations of laminar flow for a two-dimensional microchannel with the same geometry as the work reviewed above. The synthetic jet was switched on by simulating the parabolic displacement of the membrane with amplitude of 40 μm at a frequency of 560 kHz. A maximum heat transfer enhancement of approximately 125% was achieved.

Most recently, similar to the work of Timchenko et al. [12] , Chandratilleke et al. [14] numerically investigated a two-dimensional microchannel cooling with a cross-flow synthetic jet. Air was used as the working fluid. The channel was 500 μm in height and 2.25 mm long. The slot synthetic jet was located at the middle of the channel length. The synthetic jet operated at 10 kHz with the amplitude up to 100 μm. They invoked unsteady Reynolds-averaged Navier-stokes equation with the shear-stress-transport k-ω turbulence model in FLUENT for the simulation. They reported 4.3 times of heat transfer enhancement with synthetic jet, and the flow pressure drop did not increase.

Jacob and Zhong [15] recently used a circular synthetic jet blowing up from a heated surface into a low-Reynolds number laminar boundary layer, and primarily studied the nature of the synthetic jet fluidic structure. They used liquid crystal surface measurements to map out the thermal footprint of the jet's impact, though they did not quantify the impact. Later on, Zhou and Zhong [16] performed a 3-D numerical simulation for the above experimental setup. Vortical structures and shear stress footprints on the wall were captured from the simulation in FLUENT.

Go and Mongia [7] conducted an experimental study on synthetic jet acting in cross-flow to a duct representing the

confined space in a typical notebook computer. The nature of the jet and bulk flow interaction was studied using particle image velocimetry. Synthetic jets were shown to slow down the bulk flow and creating "dead zones" where the bulk flow was blocked. The heat transfer studies indicate that cooling can be increased in the main body of the synthetic jet stream by as much as 25% but that the jet creates an impediment to the bulk flow which results in other areas of localized heating.

From these works reviewed above, it shows that synthetic jets can be used to efficiently enhance heat transfer performance while interacting with pre-existing flow. However, for the microchannel cooling combines with cross-flow synthetic jet cooling, the very limited numerical works reviewed above shows considerable discrepancy with each other by employing different computational models. The degree of heat transfer enhancement for this hybrid cooling scheme needs to be experimentally examined first.

Confined by the microchannel geometry, the synthetic jet orifices geometry should be micro-holes or micro-slots. To experimentally investigate this cooling configuration using single-phase water, we overcame the challenge to form synthetic water jet through a micro hole by vibrating a piezoelectric actuator. By imposing the jet actuator perpendicularly onto a microchannel, the effect of synthetic jet on the thermal performance of microchannel can be explored experimentally. Several parameters such as membrane oscillation driving frequency, driving voltage of the jet actuator as well as the bulk microchannel flow rate are studied. The change of pressure drop across the channel and the averaged Nusselt number of microchannel for cases with/without jet are compared.

2. EXPERIMENTAL APARATUS

The experimental setup, as shown in Figure 1, consists of a water supply loop, a microchannel heat sink test section integrated with synthetic jet, a data acquisition system, and a signal generation system to drive the jet actuator.

2.1. Water flow loop

The water flow loop is configured to supply constant flow rate of deionized water to the test section. It is an open flow loop which begins with nitrogen pressurized aluminum water tank. As water flows out, the water pressure at the tank outlet will keep dropping since the tank water level keep going down even though the nitrogen pressure is constant. To keep the water outlet pressure constant, a feedback control system is designed to frequently add water into the pressure tank to keep the water level constant. The feedback system includes a pressure sensor and a controllable solenoid valve and it is controlled through LabVIEW. This gives a water outlet pressure variation less than 70 Pa. A 2 micro inline filter follows the pressure tank. After the filter, water is a degassed through a membrane degasser. The next item in the flow loop is a rotameter type flow meter. It has a flow range of 0.2 mL/min to 36 mL/min. Following the rotameter, a precision flow control valve is used to adjust the loop flow rate. Then water flows through the microchannel test section. Water drained out from the test section is ducted into a container put on a high precision balance, which is employed to further calibrate the mean flow rate.

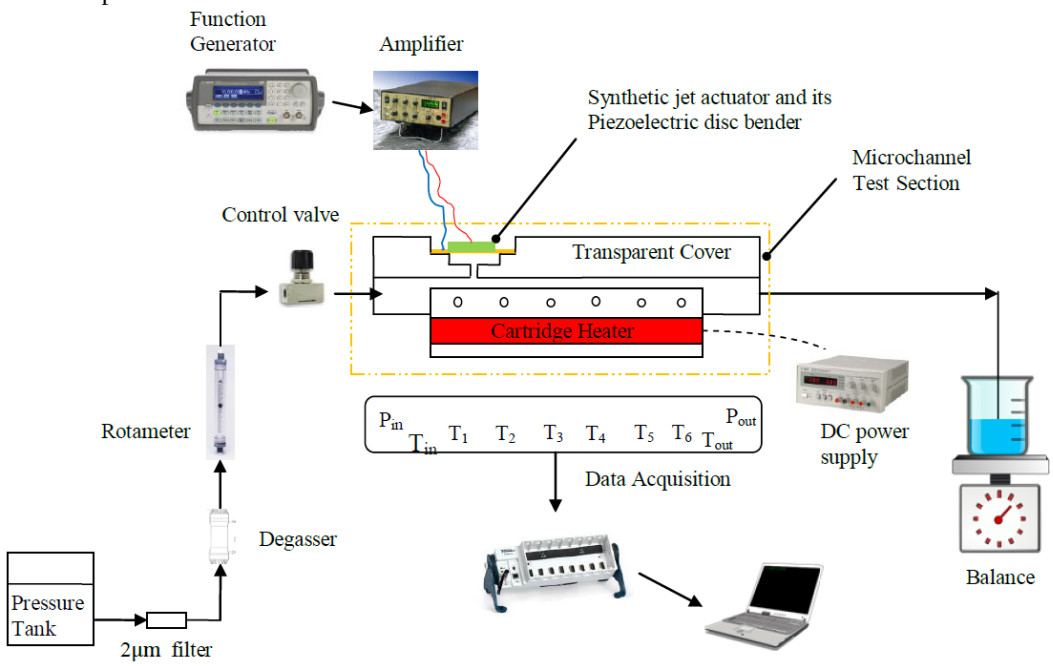

Figure 1 Schematic of flow loop and test section

2.2. Test Section

The test section assembly is illustrated in Figure 2. It consists of a cover plate with a synthetic jet cavity on it, a housing, a microchannel heat sink, a cartridge heater, insulation blocks, a support plate and a piezoelectric disk bender actuator.

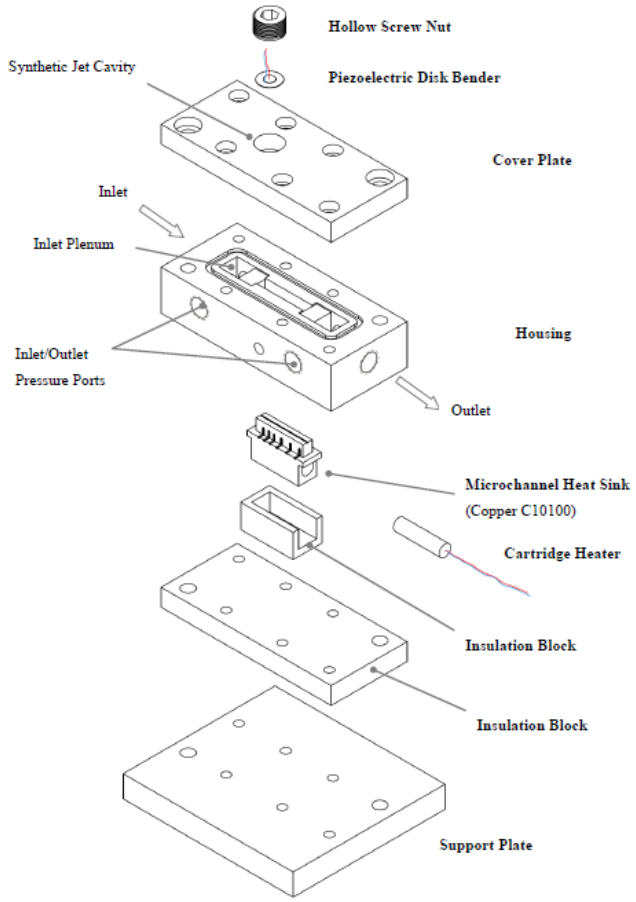

Figure 2 Test section exploded view

The microchannel heat sink part is fabricated on a single copper block. The copper is an Oxygen-Free Electronic alloy number C10100. It has a thermal conductivity of 391 W/m·K at room temperature. The top surface of the copper block measures 5 mm wide and 26 mm long. A single microchannel is machined into the copper block top surface. The channel is in the middle of the top surface and has a cross-sectional dimension of 550 μm wide and 500 μm deep. 3 mm below the top surface of the heat sink, six holes with diameter of 0.85 mm are drilled into the side wall up to the half width of the copper block. Six type-K thermocouples with a 0.8 mm bead diameter are inserted into these holes to measure the heat sink's stream-wise temperature distribution. The thermocouples are denoted in Figure 1 as T_1 to T_6 from upstream to downstream. The locations, as measured from the inlet of the microchannel and along its length, are 4 mm, 3 mm, 3 mm, 4 mm, 5 mm, and 5mm. Below the thermocouple holes, a small protruding platform is machined around the periphery of the heat sink to both facilitate accurate positioning the heat sink in the housing and to ensure adequate area for sealing. Below the platform, a 6.35 mm diameter through hole is drilled along the length of the cooper block to accommodate the cartridge heater. The resistive cartridge heater is powered by an Agilent DC power supply and provides a constant heat flux to the copper block. Power supplied to the cartridge heater is calculated based on the voltage and current readings from the DC power supply.

The housing part is made from high temperature polycarbonate plastic. The design is referred to the similar part of Qu and Mudawar [17]. The central part of the housing is removed where the heat sink can be inserted. The protruding portion of the heat sink ensured that the top surface of the heat sink is flush with the top surface of the housing. RTV silicon rubber is applied along the interface between the housing and the heat sink to prevent leakage. Two absolute pressure transducers are connected to the deep portion of inlet and outlet plenums via pressure ports to measure the inlet and outlet pressure, respectively. Two type-K thermocouples are located 1 mm away from the inlet and outlet of the microchannel to measure the channel inlet/outlet water temperatures.

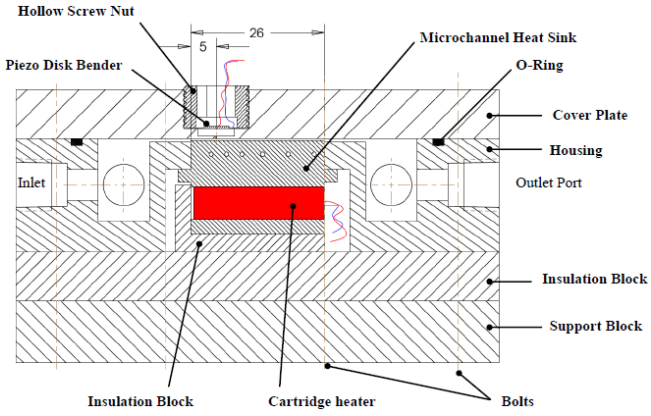

Figure 3 Test section assembly

The cover plate made from transparent polycarbonate plastic is bolted atop the housing. The cover plate and the micro-slot in the heat sink top surface form closed microchannel as shown in Figure 3. An O-ring in the housing maintains a leak-proof assembly.

The synthetic jet actuator is located right above the microchannel and 5 mm downstream from the microchannel inlet, as shown in Figure 3 and Figure 4. It is formed by a cylindrical cavity, a 100 μm diameter orifice on the cavity

bottom surface, and a vibration membrane on the cavity top surface. The cylindrical jet cavity has a diameter of 9.6 mm and 1.5 mm in depth. It is machined into the cover plate. The orifice is drilled through the bottom surface of the cavity, which is 0.5 mm in thickness.

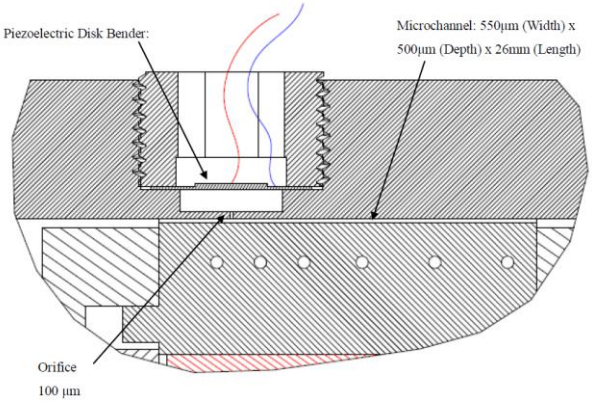

Figure 4 Enlarged view of synthetic jet assembly

In this study, a Unimorph piezo element is employed as the actuator. A Unimorph disk is made of two disks bonded together, one is a piezoelectric ceramic the other is metal substrate. Silver electrode is coated on the piezoelectric ceramic surface. The disk bows up or down as a voltage is applied between the metal disk and the silver electrode. The metal disk makes it much less fragile than the ceramic alone. In this case, the metal substrate is a thin brass disc, which has a diameter of 12 mm and a thickness of 100 μm, the piezoelectric ceramic disk has a diameter of 9 mm and a thickness of 100 μm. The resonance frequency of the piezo disk bender itself is 9 kHz. After assembly, the synthetic jet actuator resonance frequency is lowered because of the damping effect of the water enclosed in the cavity.

During assembly, the piezoelectric disk bender is placed on top of the cylindrical cavity coaxially to seal it. The periphery of the disk bender is tightly fixed by a hollow screw nut. Electrical wires which are connected to the silver electrode and the brass disc stretch out from the hollow screw nut.

2.3. Data acquisition and signal generation systems

A NI CompactDAQ-9172 data acquisition system is employed to record signals from the two pressure transducers and eight thermocouples. The system communicates with a computer via a USB interface. A program written in LabVIEW software is used for all data acquisition. The sample rate for the thermocouples is 1 S/s and 1 KHz for the two pressure transducers.

The signal generation system is designed to supply sinusoidal signal to drive the piezoelectric disk actuator. It includes a direct digital synthesis function generator, a wide band power amplifier and a digital oscilloscope. It is capable of generating sine wave with the frequency from 1 Hz to 7 MHz, and the amplitude up to 200 volts (p-p).

2.4. Measurement uncertainty

The accuracy of pressure transducer, thermocouple, and Agilent E3612A DC power supply are 0.25%, ±0.2°C, ±0.01V, and 0.5% respectively. The rotameter has an advised flow accuracy of 2.0%. However, the measured accuracy is actually less than 1%. The sine wave flatness of the function generator is 1.0% and the output peak voltage accuracy of the amplifier is given by ±0.5V.

3. EXPERIMENTAL PROCEDURE AND DATA POST PROCESSING

3.1. Experimental procedure

The experiment procedure is as follows, for the conduct of each test. Once the test section is assembled, the whole test section except the water supply tubes is put into a foam box for further insulation. The desired flow rate for each test run is set constant using the flow control valve. After the flow rate stabilize, the heater power supply is switched on and maintained at the required level by setting a constant voltage of the DC power supply, and a steady state is usually reached in 90-120 min. LabVIEW software is used as the data acquisition system and to monitor temperatures of all of the thermocouples and pressure transducers. Steady state is considered to be achieved when the 100 readings averaged temperature of the thermocouples remains constant over a fifteen-minute time interval. 600 data points for each of the thermocouple readings are collected after the system reaches steady state. Also recorded are the pressure transducer readings, flow rate and heating power. The recordings are repeated for 3 times with a 5 minutes interval.

For each test case with synthetic jet, the function generator and the amplifier are set to output sinusoidal signal at desired frequency and amplitude, keeping the flow rate unchanged, and then switching on the synthetic jet. The temperatures of the microchannel heat sink will drop immediately after the jet opens. Another steady state will be achieved in around 60 minutes. The above recording process is repeated for each of the test cases.

3.2. Data post processing

The average heat transfer coefficient is determined from the basic convective heat transfer equation shown in Eq. (1).

$$\bar{h} = q/[A_{ht} \cdot \Delta T_{LMTD}] \quad (1)$$

Where q is the heat transfer rate, A_{ht} is the heat transfer area, and ΔT_{LMTD} is the log mean temperature difference given by Eq. (2).

$$\Delta T_{LMTD} = \frac{(T_s - T_i) - (T_s - T_o)}{\ln\left({}^{T_s - T_i}/_{T_s - T_o}\right)} \quad (2)$$

Where T_s is the surface temperature, T_i is the inlet fluid temperature, and T_o is the outlet fluid temperature. T_i and T_o are obtained from the averaged readings of inlet/outlet thermocouples. A_{ht} is the summation of the three microchannel wall surface areas. The heat transfer rate, q, can be determined from Eq. (3).

$$q = \rho Q(h_o - h_i) \quad (3)$$

Where the water volumetric flow rate Q is measured with the rotameter. The inlet and outlet fluid enthalpies are obtained from NIST by knowing the water inlet/outlet conditions: T_i, P_i and T_o, P_o. The density is calculated based on mean bulk water temperature.

As direct measurements of the microchannel wall surface temperature were not available, the microchannel surface temperature T_s is determined from the thermocouple readings from Eq. (4).

$$T_{s,j} = T_j - s \cdot q/(k_{cu} \cdot A_{lm}) \quad (4)$$

Where $T_{s,j}$ is the local wall surface temperature corresponding to the imbedded thermocouples, T_j is each thermocouple reading, s is the distance from the thermocouples to the microchannel bottom wall surface, which is 2.5 mm in this case, k_{cu} is the copper heat conductivity, and T_s is the average of $T_{s,j}$. Heat conduction across the walls of a single rectangular channel is more complicated to evaluate compare to a heat sink with multichannel, since the heat transfer surface area is continuously decreasing towards the channel. Analog to heat transfer across a tube wall, a log mean cross-section area, A_{lm}, is defined as following:

$$A_{lm} = \frac{A_{outer} - A_{ht}}{\ln\left(A_{outer}/A_{ht}\right)} \quad (5)$$

Where A_{outer} is the section area where the thermocouples are located. Due to the high thermal conductivity of copper, the uncertainty involved with such an estimation of the wall temperature is small.

Finally, the corresponding average Nusselt number is calculated from Eq. (6).

$$\overline{Nu} = \bar{h}D_h/k_f \quad (6)$$

In which the thermal conductivity k_f of water is evaluated at the mean fluid temperature, and $D_h = 0.53$ mm.

The Reynolds number is based on the inlet parameters.

$$Re = QD_h/\nu A_{ch} \quad (7)$$

Where ν is the kinematic viscosity evaluated based on inlet fluid conditions T_i and P_i. A_{ch} is the channels cross-section area and Q is water volume flow rate.

4. RESULTS AND DISCUSSION

The effects of synthetic jet on the heat transfer performance of microchannel are investigated based on the following three parameters: the microchannel flow Reynolds number, the jet actuator operating frequency and the operating voltage. Also the effect of synthetic jet on the microchannel pressure drop is measured and reported in this section. All tests are conducted with the same electrical power supplied to the cartridge heater. It is measured at 7.0 Watts. Heat transferred to water depends on the microchannel flow rate, for the Remolds number above 400, around 90% percent of the heat is absorbed by water.

4.1. $\overline{Nu}$ vs. Re

The results reported in Figure 5 shows the thermal enhancement of synthetic jet on microchannel heat transfer for cases with/without jet at different Reynolds number. The synthetic jet actuator is operated at 80Hz, with the driving voltage of 60Vp.

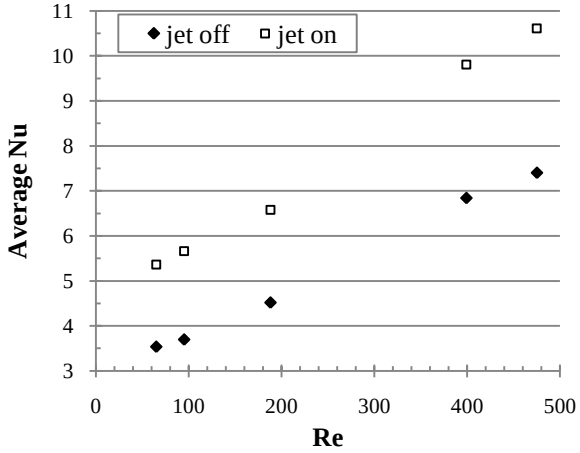

Figure 5 The effects of Reynolds number on heat transfer performance. V = 60Vp, frequency=80Hz

As shown in the above figure, for the microchannel heat transfer without jet, the average Nusselt is a function of Reynolds number rather than a constant value as predicted for fully developed duct flow heat transfer. This discrepancy is explained by several researchers such as Steinke and Kandlikar [18], Lee and Garimella [19]. It is mainly because the flow regime is thermally developing rather than fully developed. Table 1 below shows the thermal development length for several test cases. Those tests fall either into a hydrodynamically developed but thermally developing or a simultaneous developing regime.

Table 1 Flow regime of the testing cases in Figure 5

$Re=Q*D_h/(\nu*A)$	/	95	188	399	475
Thermal entry length $L= 0.05D_hRePr$	mm	11.1	24.1	53.5	65.9

When the synthetic jet is switched on, the heat transfer coefficient is enhanced. For the case of Re = 95, around 53% enhancement is achieved under the specified operating conditions based on the averaged Nu. While for microchannel flow at higher Reynolds number, Re = 475, the relative augmentation is around 42%. This is expected

since for the flow at lower flow rate, the laminar boundary layer is thicker at the same location compared to that at higher flow rate. Consequently, the interruption of a thicker laminar boundary layer will generate relatively higher heat transfer enhancement. We can expect that the synthetic jet will have even higher effect on the microchannel heat transfer performance if the microchannel flow is fully developed both thermally and hydraulically, since the laminar boundary layer reaches its maximum thickness under that situation.

4.2. $\overline{Nu}$ *vs. jet driving voltage*

One obvious way to control the synthetic jet strength is to change the vibration amplitude of the actuator. Change in the voltage will change the deformation of the disk bender directly. In general, there is a linear relationship between the voltage and the deformation for piezoelectric materials.

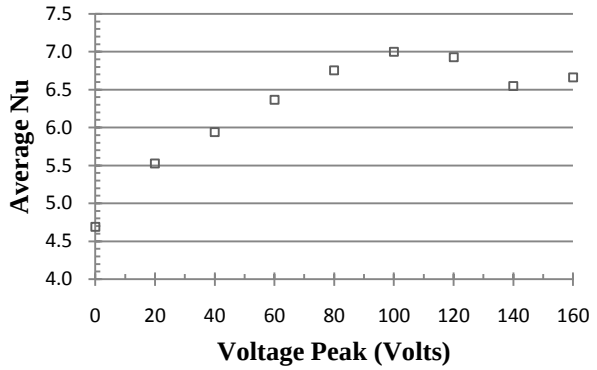

Figure 6 The effects of piezo actuator driving voltage on heat transfer performance. Re = 188, frequency = 80Hz

Figure 6 shows the effects of driving voltage of the piezo disc actuator on the microchannel heat transfer performance. There is an almost linear relationship for the voltage up to 90Vp. It seems that the jet reached its maximum capacity in the range of 90Vp to 110Vp. Further increase in the voltage to 120Vp leads to partially lower heat transfer coefficient. It is very likely that part of the piezo disk bender is depolarized when the voltage exceeds 120Vp. Exposure to a strong electric field, of polarity opposite that of the piezoelectric ceramic element polarizing field, will depolarize a piezoelectric material [20]. Since the applied voltage, i.e., 120Vp is above the maximum allowable voltage of the actuator, the depolarization may be responsible for the degradation of the performance of the synthetic jet.

4.3. $\overline{Nu}$ *vs. jet driving frequency*

Another way to effectively control the synthetic jet is to change its driving frequency. Changing the frequency will change the strength of the synthetic jet as more electrical energy is transformed into mechanical energy by the piezo actuator, and as the result, the momentum transferred into the microchannel flow is changed. Second, the disturbance frequency is changed and the way to affect the main stream fluid is alternated.

Figure 7 below shows the effects of driving frequency of the piezo disc actuator on the microchannel heat transfer performance. Tests were performed from 10 Hz up to 150 Hz under the condition of constant flow rate and constant piezo actuator driving voltage for all test cases. The thermal effect of the synthetic jet increases as the frequency changes from 10Hz to 100Hz. It seems that the jet reaches its maximum capacity when the frequency is further increase up to 150Hz.

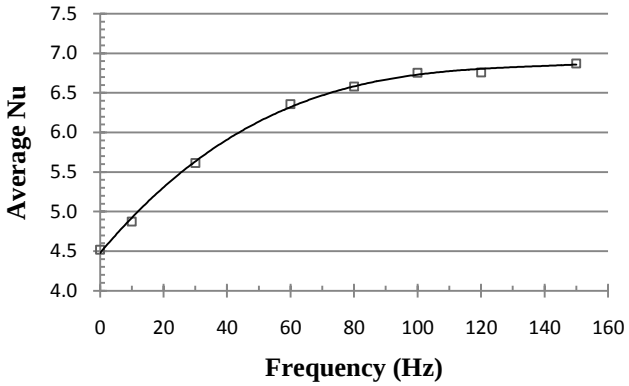

Figure 7 The effects of piezo actuator driving frequency on heat transfer performance. Re = 188, V=60Vp

The synthetic jet actuator is driven at the forced frequency rather than its resonance frequency. It's expected that we can get much higher oscillation amplitude of the disk bender if it is driven near the natural frequency of the device, and thus get higher thermal impact on the microchannel heat transfer. We will explore this possibility in the future.

4.4. *Synthetic jet effects on the microchannel heat sink local temperature*

Temperature variations of the microchannel heat sink along the length with and without synthetic jet for one test case are compared and presented in Figure 8. The flow condition and jet operation parameters are listed in the figure. The heat sink temperatures denoted in the plot are the measured temperatures of the six thermocouples, which are located 2.5 mm below the microchannel bottom surface.

As expected, the copper temperature distribution along the microchannel length is linear without synthetic jet. For this test case, the rise is around 0.8 ^{o}C from T_1 to T_6. As the synthetic jet is switched on, the heat sink copper temperatures drop about 4.3 ^{o}C as shown in Figure 8, while the inlet and outlet water temperatures keeps almost the same. It's noted that the temperature distribution is still linear along the channel length. The local impingement

cooling effect on the heat sink of the synthetic jet is not very obvious since it is spread rapidly along the heat sink because of the high heat conductivity of copper.

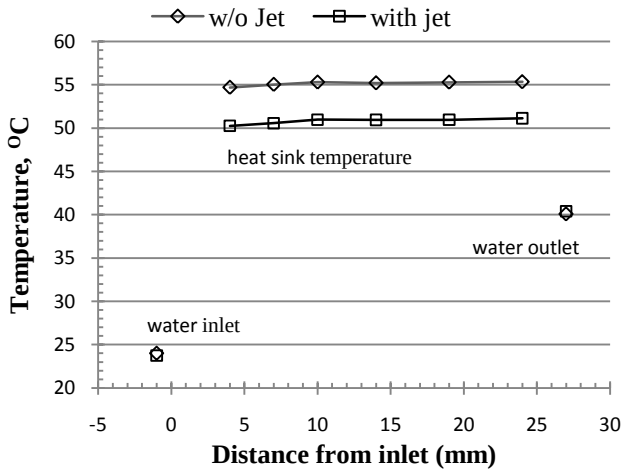

Figure 8 Temperature variations with and without synthetic jet. Re = 190, V=60Vp, frequency = 80Hz

However, the measured heat sink temperature difference between the thermocouples T_2 and T_3 reveals that the jet impingement does have effects on the change of local temperature of the cooper heat sink near the jet opening, though not much. The differences for several test cases are summarized in Table 2.

Table 2 heat sink temperature variation near the jet

Re	/	65	95	137	188
$\Delta T = T_3 - T_2$ Without jet	°C	0.29	0.29	0.27	0.26
$\Delta T = T_3 - T_2$ With jet	°C	0.51	0.47	0.44	0.41

4.5. *Pressure drop*

The results reported in Figure 9 shows the pressure drop change with and without synthetic jet for several test cases.

They are also compared with conventional theory based on the Navier-Stokes equation for laminar fully developed flow through the rectangular microchannels. The friction factor is given by $fRe = C(\gamma)$, where the constant C depends on the aspect ratio γ only. For this particular microchannel, C is around 14.5. The measured pressure drops have a good agreement with the theory for lower Reynolds numbers. For the Reynolds number greater than 200, the measured pressure drop begin to deviate from the prediction of the conventional theory, since the flow regime is more in the developing region rather than fully developed.

As shown in the figure, when the synthetic jet is open, the pressure drops across the microchannel will increase slightly. It is around 70 Pa increase reading from the pressure transducers for the test cases reported here. This feature highlights the merit of this cooling scheme that it can enhance the microchannel heat transfer performance with the pressure drop increasing very slightly.

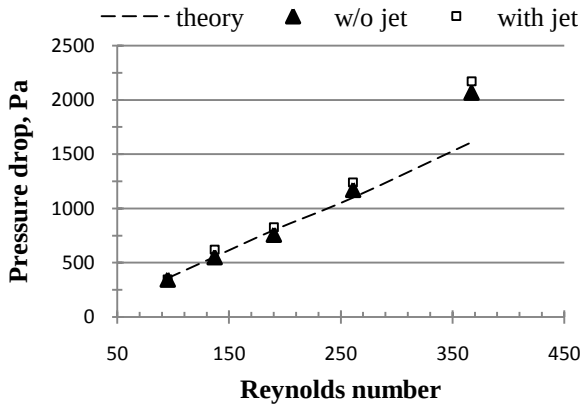

Figure 9 Effect of synthetic jet on pressure drop. V = 60Vp, frequency = 80Hz

4.6. *Joule heating of the piezo element*

The power used to drive the piezo actuator is measured to quantify the joule heating effect caused by the piezo element. The results show that the joule heating effect is negligible. For a typical test case, where the piezo is driving at 60 volts (peak) and 60 Hz, the electrical power input is measured at 0.05 Watts. That's negligible compared to the heating power supplied to the cartridge heater even if all the actuator driving power is turned into heat.

5. CONCLUSION

The present work experimentally investigated the thermal effects of a synthetic jet actuator on the heat transfer performance of single-phase water flow confined in a microchannel heat sink. The effects of the bulk microchannel flow Reynolds number, the synthetic jet operating voltage and frequency on the microchannel heat transfer performance are being investigated respectively.

The thermal effects of the synthetic jet are a function of the flow Reynolds number. It shows that the jet has a bigger improvement on heat transfer performance for the lower microchannel flow rates. For the case of Re = 95, around 53% enhancement is achieved under the specified operating conditions.

The thermal effects of the synthetic jet can be adjusted by changing the actuator driving voltage and/or frequency. Increasing the driving voltage or frequency, up to certain threshold value respectively, will increase the microchannel heat transfer performance.

Though we can detect small temperature changes near the jet orifice, the local impingement cooling effect of the synthetic jet is not very obvious because of the high heat conductivity of the heat sink.

We found that this hybrid cooling scheme can enhance the heat transfer performance at a very small penalty of pressure drop increase across the microchannel.

Given the fact that one micro-synthetic jet can only effectively affect a small portion of the microchannel, we can expect to have a promising heat transfer enhancement if multi-jets are applied along the microchannel.

6. ACKNOWLEDGMENTS

The authors acknowledge support for this research from the Office of Naval Research under ESRDC consortium, program managed by Terry Ericsen.

7. REFERENCES

[1] Sung, Myung Ki and Issam, Mudawar. ,Experimental and numerical investigation of single-phase heat transfer using a hybrid jet-impingement micro-channel cooling scheme. International journal of heat and mass transfer. 2006, Vol. 49, pp. 682-694.

[2] Bergles, A.E. ,ExHFT for Fourth Generation Heat Transfer Technology. Experimental Thermal Fluid Science. 2002, Vol. 26, pp. 335-344.

[3] Tuckerman, D.B. and Pease, R.F.W. ,High-performance heat sinking for VLSI. IEEE Electron Device Letters. 1981, Vols. EDL-2, pp. 126-129.

[4] Steinke, M.E. and Kandlikar, S.G. ,Single-phase heat transfer enhancement techniques in microchannel and minichannel flows. ICMM. Rochester, New York, USA, June 2004.

[5] Colgan, E.G., et al. ,A Practical Implementation of Silicon Microchannel. Coolers for High Power Chips. Semiconductor Thermal Measurement and Management Symposium, 2005 IEEE Twenty First Annual. 2005 March 15-17, pp. 8-15.

[6] Glezer, A. and Amitay, M. ,Synthetic Jets. Annual Review of Fluid Mechanics. 2002.34:503-29.

[7] Go, D.B. and Mongia, R.K. ,Experimental studies on synthetic jet cooling enhancement for portable platforms. Thermal and Thermomechanical Phenomena in Electronic Systems. 2008, pp. 528-536.

[8] Smith, B.L. and Glezer, A. ,Jet vectoring using synthetic jets. Journal of Fluid Mechanics. 2002, Vol. 458, pp. 1-34.

[9] Amitay, M, et al. ,Modification of the aerodynamic characteristics of bluff bodies using fluidic actuators. AIAA. 97-2004.

[10] Crook, A, Sadri, AM and Wood, NJ. ,The development and implementation of synthetic jets for the control of separated flow. AIAA. 99-3176.

[11] Mahalingam, R and Glezer, A. ,Design and thermal characteristics of a synthetic jet ejector heat sink. Journal of Electronic Packaging. 2005, Vol. 127, pp. 172-177.

[12] Timchenko, V, Reizes, J and Leonardi, E. ,Numerical Study of Enhanced Micro-channel Cooling Using a Synthetic. 15 th Australasian Fluid Mechanics Conference. Sydney, Australia,Dcember 2004.

[13] Timchenko, V, et al. , Heat Transfer Enhancement using Synthetic Jet Actuators in Forced Convection Water Filled Micro-Channels. Proceedings of the 3rd IASME/WSEAS Int. Conf. on Heat Transfer, Thermal Engineering And Environment, Corfu, Greece,. August 20-22,2005, pp. 294-299.

[14] Chandratilleke, T.T., Jagannatha, D. and Narayanaswamy, R. Heat transfer enhancement in microchannels with cross-flow synthetic jets. International Journal of Thermal Sciences. 2009, Vol. 49, pp. 504-513.

[15] Jabbal, M. and Zhong, S. ,The near wall effect of synthetic jets in a boundary layer. International Journal of Heat and Fluid Flow. 2008, Vol. 29, pp. 119-130.

[16] Zhou, Jue and Shan Zhong. ,Numerical simulation of the interaction of a circular synthetic jet with a boundary layer. Computers & Fluids. 2009, Vol. 38, pp. 393-405.

[17] Qu, W. and Mudawar, I. Experimental and numerical study of pressure drop and heat transfer in a single-phase micro-channel heat sink. Int. J. Heat Mass Transfer. June 2002, Vol. 45, pp. 2549-2565.

[18] Steinke, Mark E. and kandlikar, Satish G. ,Single-phase Liquid heat transfer in Microchannels. 3rd International conference on Microchannels and Minichannels. Toronto,Canada, June 13-15,2005.

[19] Lee, Poh-Seng and Garimella, Suresh V. ,Thermally developing flow and heat transfer in rectangular microchannels of different aspect ratios. International Journal of Heat and Mass Transfer. 2006, Vol. 49, pp. 3060-3067.

[20] http://www.americanpiezo.com/piezo_theory/behavior.html.